Assessment of Glaucomatous Changes in Subjects with High Myopia Using Spectral Domain Optical Coherence Tomography

Takuhei Shoji,[1,2] Hiroki Sato,[3] Masahiro Ishida,[1] Masaru Takeuchi,[1] and Etsuo Chihara[2]

Purpose. To evaluate the diagnostic ability to detect glaucoma in highly myopic eyes using spectral domain–optical coherence tomography (SD-OCT) parameters in a cross-sectional comparative study.

Methods. A total of 82 patients with high myopia (≤ -5 D) presented between April 2008 and August 2009. Subjects comprised 31 participants with high myopia but not perimetric glaucoma (no glaucoma group) and 51 patients with high myopia and concomitant perimetric glaucoma (glaucoma group). Ganglion cell complex (GCC), circumpapillary retinal nerve fiber layer (p-RNFL), and disc configuration parameters were obtained from algorithms of the SD-OCT system and subsequently compared. Receiver operating characteristics curves were constructed for each measurement parameter, and areas under the curves (AUCs) were compared.

Results. All optic nerve fiber head, except disc area, and GCC parameters differed significantly between groups ($P < 0.05$). The largest AUCs from disc configuration, circumpapillary RNFL, and GCC parameters were 0.844 (C/D vertical), 0.826 (RNFL average), and 0.954 (global loss volume [GLV]), respectively. GLV was significantly better for detecting perimetric glaucoma than both the C/D vertical and RNFL average ($P < 0.05$).

Conclusions. All algorithms of the OCT system were useful for discriminating glaucoma. Among these, GCC measurements offered the best parameters for the clinical diagnosis of glaucoma in patients with high myopia and concomitant perimetric glaucoma. (*Invest Ophthalmol Vis Sci.* 2011;52:1098–1102) DOI:10.1167/iovs.10-5922

Myopia is an independent risk factor for glaucoma.[1,2] Past epidemiologic studies described that subjects with myopia show a two- to threefold increase in the risk of developing glaucoma compared with nonmyopic eyes, and the risk of developing glaucoma increases with increasing degree of myopia.[1,2] Once pathology is present, deterioration of the visual field may be enhanced,[3] and macular functions may be selectively impaired in patients with both high myopia and glaucoma.[4,5] Early diagnosis and management in such patients is thus crucial. However, diagnosis of glaucoma in highly myopic eyes is not easy. Tilting, large ovalness index, deformation of the disc,

pale disc, shallow and large cup, large peripapillary crescent, and occasional optic disc hypoplasia of highly myopic subjects hamper precise diagnosis of glaucoma.[6,7]

Until recently, retinal nerve fiber layer (RNFL) analyzers, including those using time-domain (TD) optical coherence tomography (OCT), scanning laser polarimetry (SLP), and Heidelberg retinal tomography (HRT) have been shown to be useful for discriminating between nonglaucomatous and glaucomatous patients. However, these discriminating abilities are significantly decreased in eyes with both high myopia and glaucoma.[8]

Recent spectral-domain (SD) imaging offers significant advantages over traditional TD-OCT techniques,[9] such as faster acquisition speed and increased depth resolution,[10] but clinicians now need to determine how the new devices can benefit glaucoma diagnosis and management in patients with high myopia.

A modern SD-OCT system (RTVue-100, software version 4.0.0.143, model RT 100; Optovue, Fremont, CA) provides a high frame-transfer rate and fast Fourier transform algorithm, can perform up to 26,000 A-scans per second with a depth resolution of approximately 5 μm, and is able to obtain cross-sectional and three-dimensional images of the RNFL, the optic disc, and the ganglion cell complex (GCC) around the fovea.[10]

However, few reports have described the use of SD-OCT in highly myopic eyes with concomitant glaucoma.[8] In the present study, an ability to detect glaucomatous changes in highly myopic eyes was compared between GCC parameters and disc configuration parameters and circumpapillary RNFL (p-RNFL) parameters.

Methods

This study was conducted on consecutive patients using the outpatient services of the Sensho-kai Eye Institute, Uji, Japan, between April 2008 and August 2009, who satisfied the inclusion and exclusion criteria. This cross-sectional study was designed to evaluate glaucomatous changes in highly myopic eyes. Informed consent was obtained from all participants, and the methods applied in the study adhered to the tenets of the Declaration of Helsinki for the use of human subjects in biomedical research. All study protocols were approved by the institutional ethics committee of Sensho-kai Eye Institute. The three algorithms of the SD-OCT system used in the present study included GCC, RNFL and three-dimensional optic disc parameters. All participants underwent a complete ophthalmologic examination, including assessment of medical and family history, visual acuity testing with refraction, slit-lamp biomicroscopy including gonioscopy, intraocular pressure (IOP) measurement with Goldmann applanation tonometry, and dilated stereoscopic fundus examination. Visual sensitivity was tested using a full-threshold (G1) program (Octopus 301; Interzeag, Schlieren, Switzerland). Inclusion criteria for all participants were the following; best corrected visual acuity, 20/40 or better; age, >40 years; spherical equivalent refraction, ≤ -5.0 D; a healthy anterior segment appear-

TABLE 1. Baseline Characteristics of No Glaucoma Group (NGG) and Glaucoma Group (GG)

	NGG (n = 31)	GG (n = 51)	P
Male, *n* (%)	12 (38.7)	27 (52.9)	0.211
Age, y	55.4 ± 13.0	53.7 ± 12.9	0.580
MD, dB	1.0 ± 2.5	8.1 ± 7.7	<0.001
Spherical equivalent error, D	−10.3 ± 4.7	−8.9 ± 3.1	0.147

Plus-or-minus values are means ± SD. Baseline characteristics were compared using the unpaired *t*-test or chi-square test, as appropriate, between the groups.

ance on examination with slit-lamp biomicroscopy; open angles at gonioscopy; and reliable visual field (VF) results. Subjects were excluded if any evidence suggested a history of ocular surgery (except for uncomplicated cataract surgery), other diseases affecting the VFs (e.g., neuro-ophthalmological diseases, uveitis, or retinal and/or choroidal diseases, trauma). For the purpose of this study, participants were categorized as showing high myopia without perimetric glaucoma (no glaucoma group [NGG]) or high myopia with concomitant perimetric glaucoma (glaucoma group [GG]). The NGG subjects were those with IOP < 22 mm Hg and normal VF results. The GG patients displayed repeatable glaucomatous abnormal VF results. Diagnosis of glaucoma depends on a glaucomatous VF defect that was defined as either a cluster of three adjacent points depressed by ≥5 dB or two independent points depressed by ≥10 dB in the "comparison" visual field.

Instrumentation

The system employed uses a scanning laser diode to emit a scan beam with a wavelength of 840 ± 10 nm to provide images of ocular microstructures. In this study, three protocols (3D Disc, ONH, and GCC RTVue-100 [Optovue]) were used. The 3D Disc protocol is a 6 × 6 mm raster scan centered on the optic disc and comprises 101 B-scans, each of which comprises 513 A-scans. The resulting scan provides a three-dimensional image of the optic disc and surrounding area. For the present study, the en face image generated by this scanning protocol was used to draw a contour line describing the disc margin required to generate optic disc parameters from the ONH protocol. The retinal pigment epithelium (RPE)/choroids endpoints, called RPE tips, were initially automatically drawn on the en face image. Trained staff can accept it without any modification or can modify them based on the en face and B scan images. The contour line was also initially automatically drawn on the en face image. In a case of temporal crescent, the assessed position of the contour line was corrected according to the brightness of the en face image in approximately eight locations.

The ONH protocol comprises 12 radial scans 3.4 mm in length (455 A-scans each) and 13 concentric ring scans ranging from 1.3 to 4.9 mm in diameter (425, 587, 775, or 965 A-scans each), all centered on the optic disc (using the previously drawn contour line to ensure scan registration). This scan configuration provides 14,141 A-scans in 0.55 seconds. Areas between A-scans are interpolated. A polar RNFL thickness map and various parameters that describe the optic disc are provided. RNFL thickness measurements were obtained for the 3.45-mm-diameter ring. RNFL thickness parameters were measured by assessing a total of 2325 data points between the anterior and posterior RNFL borders. The optic cup is automatically defined by the system software as the intersection points of the nerve head (ONH) inner boundary and a parallel line 150 μm above the line connecting each RPE tip.

The GCC scan measures retinal thickness between the posterior boundary of the inner plexiform layer and anterior boundary of the retinal nerve fiber layer and comprises one horizontal line and 15 vertical lines at 0.5 mm intervals; the center of the GCC scan is shifted 0.75 mm temporally to improve sampling of the temporal periphery.

Global Loss Volume and Focal Loss Volume

Global loss volume (GLV) and focal loss volume (FLV) are two new parameters for the GCC scan in the 4.0 software. GLV measures the average amount of GCC loss over the entire GCC map, based on the fractional deviation (FD) map. This value is the sum of individual deviation values at each pixel where the FD map value is <0, which is then divided by the total area to give an average percentage loss of GCC thickness. FLV measures the average amount of focal loss over the entire GCC map and is based on both the FD map and the pattern deviation (PD) map. The PD map is determined by first calculating the individual pattern maps from all individuals in the normative database. A PD map can be calculated by subtracting the individual's pattern map from the normative database pattern map. The statistical significance of this difference can be determined, and each pixel can be assigned a probability value based on this difference. FLV can be calculated by summing deviation map values at pixels where the FD value is <0, and the pattern deviation map value is significant ($P < 0.05$). After summing FD values at pixels, the result is divided by the total area.

Images with Signal Strength Indicator

Images with signal strength indicator (SSI) < 40 (as suggested by the manufacturer) were excluded from the analysis.

Statistical Analysis

Baseline characteristics were reported in counts and proportions or mean ± SD (SD) values as appropriate. Univariate comparisons between the groups were made with χ^2 tests or unpaired *t*-tests as appropriate. OCT parameters were reported as mean ± SD, and two groups were compared using the unpaired *t*-test. Receiver operating characteristic (ROC) curves were constructed for GCC, Disc configuration, and p-RNFL parameters for diagnosing glaucomatous eyes by plotting sensitivity versus one-specificity, and the area under each ROC curve (AUC) was calculated. Sensitivity at three levels of specificity (0.8, 0.9, 0.95) for each parameter was also calculated. To compare diagnostic algorithms, the parameters with the largest AUC were selected from GCC, 3D Disc, and RNFL algorithms, respectively. Statistical analyses comparing the largest ROC curve of GCC with that of 3D Disc and RNFL were performed using the method of DeLong et al.[11]

TABLE 2. Comparison of System Parameters in Each Group

	NGG	GG	P
GCC parameters			
Avg. GCC, μm	96.88 ± 11.24	73.53 ± 9.81	<0.001
Sup. GCC, μm	99.09 ± 11.55	76.96 ± 11.11	<0.001
Inf. GCC, μm	94.78 ± 12.60	70.15 ± 10.41	<0.001
FLV, %	3.19 ± 3.85	8.57 ± 4.46	<0.001
GLV, %	6.46 ± 6.01	24.82 ± 8.58	<0.001
ONH parameters			
Disc parameters			
Disc area, mm²	1.62 ± 0.55	1.66 ± 0.62	0.976
Cup area, mm²	0.69 ± 0.58	1.11 ± 0.52	0.001
Rim area, mm²	0.92 ± 0.47	0.51 ± 0.45	<0.001
Rim volume, mm³	0.13 ± 0.10	0.04 ± 0.04	<0.001
Nerve head volume, mm³	0.24 ± 0.17	0.10 ± 0.12	<0.001
Cup volume, mm³	0.15 ± 0.15	0.25 ± 0.23	0.029
C/D ratio, area	0.39 ± 0.29	0.70 ± 0.20	<0.001
C/D horizontal	0.58 ± 0.37	0.87 ± 0.13	<0.001
C/D vertical	0.54 ± 0.35	0.89 ± 0.10	0.001
RNFL parameters			
RNFL avg., μm	93.90 ± 13.67	77.48 ± 10.88	<0.001
RNFL sup., μm	93.52 ± 16.56	78.14 ± 13.10	<0.001
RNFL inf., μm	93.23 ± 14.38	76.79 ± 11.58	<0.001

Plus-minus values are means ± SD. Baseline characteristics were compared using the unpaired *t*-test. avg., average; inf., inferior; sup., superior.

TABLE 3. AUCs and Sensitivities at Fixed Specificities for Classifying Eyes as Healthy or Glaucomatous Using System Parameters

Parameters	AUC ± SE	Sensitivity at 0.80 Specificity	Sensitivity at 0.90 Specificity	Sensitivity at 0.95 Specificity
GCC parameters				
Avg. GCC, μm	0.954 ± 0.025	0.968	0.903	0.871
Sup. GCC, μm	0.939 ± 0.026	0.935	0.806	0.581
Inf. GCC, μm	0.935 ± 0.033	0.903	0.871	0.839
FLV, %	0.849 ± 0.047	0.843	0.588	0.235
GLV, %	0.957 ± 0.023	0.961	0.882	0.784
ONH parameters				
Disc parameters				
Disc area, mm^2	0.526 ± 0.065	0.275	0.118	0.118
Cup area, mm^2	0.705 ± 0.061	0.490	0.216	0.098
Rim area, mm^2	0.805 ± 0.048	0.710	0.226	0.065
Rim volume, mm^3	0.821 ± 0.046	0.645	0.516	0.452
Nerve head volume, mm^3	0.780 ± 0.050	0.548	0.484	0.161
Cup volume, mm^3	0.650 ± 0.066	0.255	0.196	0.196
C/D ratio, area	0.800 ± 0.049	0.627	0.529	0.294
C/D horizontal	0.767 ± 0.054	0.510	0.471	0.412
C/D vertical	0.844 ± 0.048	0.706	0.490	0.353
RNFL parameters				
RNFL avg., μm	0.826 ± 0.056	0.871	0.677	0.226
RNFL sup., μm	0.791 ± 0.058	0.710	0.613	0.323
RNFL inf., μm	0.811 ± 0.056	0.806	0.774	0.323

Statistical analyses were performed using analytical software (SAS, version 9.1; SAS Institute Inc., Cary, NC). $P < 0.05$ denotes a statistically significant difference.

RESULTS

One eye each of the 90 highly myopic participants were categorized as NGG (33 subjects) or GG (57 patients), respectively. Two NGG subjects and six GG patients were excluded because of low SSI scores. Thus, a total of 82 individuals were included in this study: 31 NGG subjects and 51 GG subjects. The characteristics of participants in both groups are summarized in Table 1.

Mean (±SD) age was 55.4 ± 13.0 years in the NGG, and 53.7 ± 12.9 years in the GG. Average refractive error (spherical equivalent refraction) was −10.3 ± 4.7 D in the NGG and −8.9 ± 3.1 D in the GG. Significant differences were seen between groups. The means of all volume and thickness parameters are listed in Table 2.

All parameters, except disc area, showed significant differences between groups ($P < 0.05$, unpaired *t*-test). Mean average GCC was 96.88 ± 11.24 μm for the NGG and 73.53 ± 9.81 μm for the GG. Mean RNFL average was 93.90 ± 13.67 μm for the NGG, and 77.48 ± 10.88 μm for the GG.

AUCs and the values of sensitivity at three levels of specificity of each parameter are listed in Table 3.

The parameters with the largest AUC for detection of glaucomatous eyes in GCC, Disc configuration, and p-RNFL parameters were GLV (AUC = 0.957; 95% confidence interval [CI], 0.911–1.00), C/D vertical (AUC = 0.844; 95% CI, 0.751–0.938) and RNFL vertical (AUC = 0.826; 95% CI, 0.715–0.937), respectively. The ROC curves of these selected parameters (GLV, C/D vertical, and RNFL average) are depicted in Figure 1. The AUC of GLV was better than that of C/D vertical (Fig. 1A, $P = 0.041$) and RNFL average (Fig. 1B, $P = 0.017$).

DISCUSSION

In this study, new parameters measuring the inner retina around the macula called the ganglion cell complex showed good ability to discriminate between glaucoma patients and nonglaucoma subjects in highly myopic subgroups.

The role of macular thickness parameters in detecting glaucoma has been previously reported,[12] as ganglion cells are
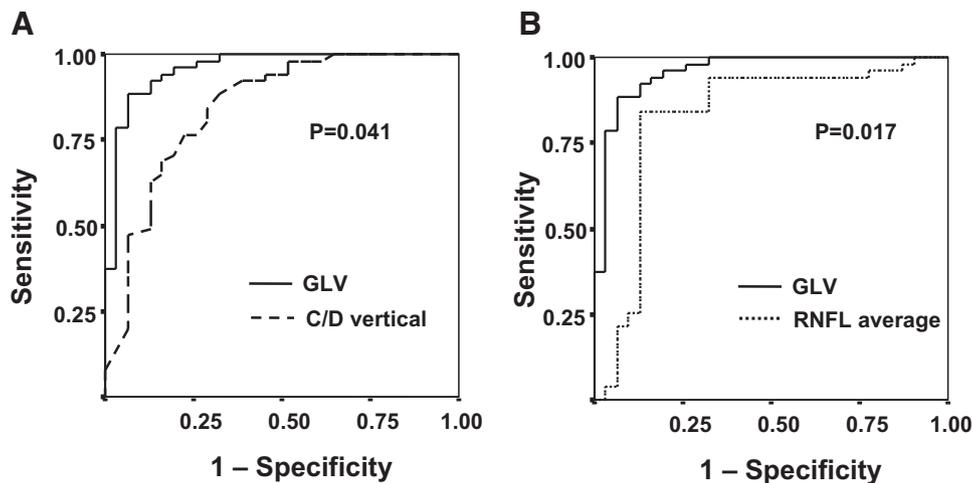

FIGURE 1. Graph showing a comparison of areas under ROC curves for the largest AUC parameters between GLV and C/D vertical (**A**) and RNFL average (**B**).

thickest at the perifovea and constitute 30%–35% of retinal thickness in this region. GCC encompasses three layers in the retina, comprising the retinal nerve fiber layer (NFL), ganglion cell layer (GCL), and inner-plexiform layer (IPL). NFL and GCL become thinner as ganglion cells die from glaucoma. Tanito et al.[13] reported that retinal thickness measurement around the macula was effective for discriminating glaucoma from normal eyes using a retinal thickness analyzer (RTA). However, posterior pole retinal thickness analysis in myopic eyes using RTA and TD-OCT yielded conflicting results.[14,15] To our knowledge, few studies have been conducted using SD-OCT in myopic eyes with concomitant glaucoma. The higher-resolution SD-OCT system allows measurement of specific segments of the retina. Measurements of the GCC, reflecting the death of ganglion cells, may improve discriminatory ability.[12,16]

Regarding p-RNFL measurement, Tan et al.[17] reported the AUCs of GCC parameters and p-RNFL measurements were similar in glaucoma detection, excluding highly myopic eyes. However, the relationship between p-RNFL measurements and degree of myopia is controversial. Hoh et al.[18] reported that the mean p-RNFL thickness did not vary with myopia or axial length, others have stated that OCT may not be reliable in the analysis of highly myopic eyes,[19,20] and recent studies reported that high myopes had different topographic profiles compared with low myopes.[21,22] Insofar as our study is concerned, AUCs for the GLV and RNFL average were 0.957 and 0.826, respectively, and the difference was statistically significant ($P = 0.017$). The present study implies that the diagnostic power of GCC parameters may overwhelm that of p-RNFL parameters in highly myopic eyes.

Optic disc configuration measurements, such as C/D vertical ratio and rim volume, are also important diagnostic parameters for glaucoma. However, a recent report indicated that the detectability of rim area measurement using HRT in glaucomatous change was inferior to that of p-RNFL parameters using SD-OCT.[23] Melo et al.[8] suggested that TD-OCT, SLP, and HRT were not useful for detecting glaucoma patients with high myopia. The optic disc of highly myopic eyes, which is frequently associated with tilting, oval configuration, and peripapillary atrophy (PPA),[24] may influence the algorithms, such as disc margin definition and scan circle size, because of a magnification effect.[25] In particular, both p-RNFL and disc parameters are severely affected by the determination of the disc margin. However, determination of disc margin appears more difficult in eyes with a myopic tilted disc. Although a recent report stated that the operator-adjusted disc-margin definition in the system employed here is not influenced by refractive error or PPA and showed high repeatability,[26] the present study indicates that not only RNFL measurements but also disc configuration parameters are statistically worse than GCC parameters. These parameters may thus be less reliable than GCC in the analysis of highly myopic eyes.

GLV and FLV, which are new parameters for the GCC algorithms, also showed nearly the same detectability as average GCC. This is another interesting result because these parameters were compared with the normative database, which does not include highly myopic eyes. The present results may imply that the influence of high myopia on GCC may be less than that on ONH parameters. Nevertheless, further research is required.

In general, the goal of a test is to detect disease with a minimum of false-negative results. An ideal "screening" test should have reasonably high specificity with very high sensitivity. In the present study, the specificity of average GCC at 80% sensitivity was 0.968, representing the optimal detectability of all parameters with this instrument (Table 3). GCC assessment might thus represent one of the best parameters for glaucoma screening in highly myopic patients.

Our study has several limitations that should be kept in mind. The first limitation is related to the design of this study. The relationship between p-RNFL measurements and degree of myopia is controversial.[8,22,27] We believe that the current normative database may not be reliable in the analysis of myopic eyes. We evaluated only highly myopic eyes, which may restrict the results. However, our results demonstrate that a specific database for highly myopic eyes could assist in differentiating highly myopic eyes with glaucoma from those without. Second, a cross-sectional study cannot show long-term changes. Several studies have reported that structural measurements provided by SD-OCT may be able to detect anatomic changes that precede irreversible functional decay.[28] Moreover, since this study is evaluating the performances of structural assessment, we diagnosed glaucoma based on only visual field criteria to avoid the bias analysis of optic configuration parameters. However, there is a potential limitation that preperimetric glaucoma patients might be categorized in the no glaucoma group. Thus, false-positive cases in the present study may detect preperimetric glaucoma or future glaucomatous changes. Glaucoma is a progressive disease, and further studies with longitudinal follow-up would be useful to fully address this limitation. Third, though the reproducibility of ONH, disc configuration parameters, and GCC measurements in normal eyes using this system has been reported,[29-31] few data from myopic eyes have been reported. Whereas our pilot data showed similar reproducibility compared to the report by Garas et al.,[31] it remains unclear whether myopia could influence the reproducibility of these measurements. The variability in highly myopic eyes may affect our results. A final limitation is that eight eyes (8.9%) were excluded because of low SSI scores. Though the detailed SSI scoring algorithms are unknown, the poor quality of images in high myopia may be attributed to abnormal disc configuration, posterior vitreous detachment (vitreous opacity), and long axial length, which may restrict the results. However, such limitations are common to all studies of this type. A previous study reported that good quality images were found using TD-OCT in only 40% of eyes in highly myopic patients.[8]

In conclusion, the GCC parameters attained higher diagnostic power than both disc configuration parameters and p-RNFL measurements for detection of high myopia with concomitant glaucoma. These parameters provide valuable information for diagnosing and assessing patients with coexisting glaucoma and high myopia.

References

 1. Mitchell P, Hourihan F, Sandbach J, Wang JJ. The relationship between glaucoma and myopia: the Blue Mountains Eye Study. *Ophthalmology.* 1999;106:2010–2015.

 2. Suzuki Y, Iwase A, Araie M, et al. Risk factors for open-angle glaucoma in a Japanese population: the Tajimi Study. *Ophthalmology.* 2006;113:1613–1617.

 3. Chihara E, Liu X, Dong J, et al. Severe myopia as a risk factor for progressive visual field loss in primary open-angle glaucoma. *Ophthalmologica.* 1997;211:66–71.

 4. Chihara E, Honda Y. Preservation of nerve fiber layer by retinal vessels in glaucoma. *Ophthalmology.* 1992;99:208–214.

 5. Chihara E, Honda Y. Multiple defects in the retinal nerve fiber layer in glaucoma. *Graefes Arch Clin Exp Ophthalmol.* 1992;230:201–205.

 6. Ozdek SC, Onol M, Gurelik G, Hasanreisoglu B. Scanning laser polarimetry in normal subjects and patients with myopia. *Br J Ophthalmol.* 2000;84:264–267.

 7. Tay E, Seah SK, Chan SP, et al. Optic disk ovality as an index of tilt and its relationship to myopia and perimetry. *Am J Ophthalmol.* 2005;139:247–252.

 8. Melo GB, Libera RD, Barbosa AS, Pereira LM, Doi LM, Melo LA Jr. Comparison of optic disk and retinal nerve fiber layer thickness in

nonglaucomatous and glaucomatous patients with high myopia. *Am J Ophthalmol.* 2006;142:858–860.

9. Leitgeb R, Hitzenberger C, Fercher A. Performance of fourier domain vs. time domain optical coherence tomography. *Opt Express.* 2003;11:889–894.

10. Chen TC, Cense B, Pierce MC, et al. Spectral domain optical coherence tomography: ultra-high speed, ultra-high resolution ophthalmic imaging. *Arch Ophthalmol.* 2005;123:1715–1720.

11. DeLong ER, DeLong DM, Clarke-Pearson DL. Comparing the areas under two or more correlated receiver operating characteristic curves: a nonparametric approach. *Biometrics.* 1988;44:837–845.

12. Zeimer RC, Khoobehi B, Niesman MR, Magin RL. A potential method for local drug and dye delivery in the ocular vasculature. *Invest Ophthalmol Vis Sci.* 1988;29:1179–1183.

13. Tanito M, Itai N, Ohira A, Chihara E. Reduction of posterior pole retinal thickness in glaucoma detected using the retinal thickness analyzer. *Ophthalmology.* 2004;111:265–275.

14. Lam DS, Leung KS, Mohamed S, et al. Regional variations in the relationship between macular thickness measurements and myopia. *Invest Ophthalmol Vis Sci.* 2007;48:376–382.

15. Zou H, Zhang X, Xu X, Yu S. Quantitative in vivo retinal thickness measurement in chinese healthy subjects with retinal thickness analyzer. *Invest Ophthalmol Vis Sci.* 2006;47:341–347.

16. Ishikawa H, Stein DM, Wollstein G, Beaton S, Fujimoto JG, Schuman JS. Macular segmentation with optical coherence tomography. *Invest Ophthalmol Vis Sci.* 2005;46:2012–2017.

17. Tan O, Chopra V, Lu AT, et al. Detection of macular ganglion cell loss in glaucoma by Fourier-domain optical coherence tomography. *Ophthalmology.* 2009;116:2305–2314 e2301–2302.

18. Hoh ST, Lim MC, Seah SK, et al. Peripapillary retinal nerve fiber layer thickness variations with myopia. *Ophthalmology.* 2006;113:773–777.

19. Leung CK, Mohamed S, Leung KS, et al. Retinal nerve fiber layer measurements in myopia: An optical coherence tomography study. *Invest Ophthalmol Vis Sci.* 2006;47:5171–5176.

20. Rauscher FM, Sekhon N, Feuer WJ, Budenz DL. Myopia affects retinal nerve fiber layer measurements as determined by optical coherence tomography. *J Glaucoma.* 2009;18:501–505.

21. Kim MJ, Lee EJ, Kim TW. Peripapillary retinal nerve fibre layer thickness profile in subjects with myopia measured using the Stratus optical coherence tomography. *Br J Ophthalmol.* 2010;94:115–120.

22. Kang SH, Hong SW, Im S, Lee S, Ahn MD. Effect of myopia on the thickness of the retinal nerve fiber layer measured by Cirrus HD optical coherence tomography. *Invest Ophthalmol Vis Sci.* 2010;51:4075–4083.

23. Leung CK, Ye C, Weinreb RN, et al. Retinal nerve fiber layer imaging with spectral-domain optical coherence tomography: a study on diagnostic agreement with Heidelberg retinal tomograph. *Ophthalmology.* 2010;117:267–274.

24. Tong L, Chan YH, Gazzard G, et al. Heidelberg retinal tomography of optic disc and nerve fiber layer in Singapore children: variations with disc tilt and refractive error. *Invest Ophthalmol Vis Sci.* 2007;48:4939–4944.

25. Leung CK, Cheng AC, Chong KK, et al. Optic disc measurements in myopia with optical coherence tomography and confocal scanning laser ophthalmoscopy. *Invest Ophthalmol Vis Sci.* 2007;48:3178–3183.

26. Garas A, Vargha P, Hollo G. automatic, operator-adjusted, and manual disc-definition for optic nerve head and retinal nerve fiber layer measurements with the RTVue-100 optical coherence tomograph. *J Glaucoma.* In press.

27. Vernon SA, Rotchford AP, Negi A, Ryatt S, Tattersal C. Peripapillary retinal nerve fibre layer thickness in highly myopic Caucasians as measured by Stratus optical coherence tomography. *Br J Ophthalmol.* 2008;92:1076–1080.

28. Tan O, Li G, Lu AT, Varma R, Huang D. Mapping of macular substructures with optical coherence tomography for glaucoma diagnosis. *Ophthalmology.* 2008;115:949–956.

29. Gonzalez-Garcia AO, Vizzeri G, Bowd C, Medeiros FA, Zangwill LM, Weinreb RN. Reproducibility of RTVue retinal nerve fiber layer thickness and optic disc measurements and agreement with Stratus optical coherence tomography measurements. *Am J Ophthalmol.* 2009;147:1067–1074.

30. Garas A, Toth M, Vargha P, Hollo G. Comparison of repeatability of retinal nerve fiber layer thickness measurement made using the RTVue Fourier-domain optical coherence tomograph and the GDx scanning laser polarimeter with variable or enhanced corneal compensation. *J Glaucoma.* 2010;19:412–417.

31. Garas A, Vargha P, Hollo G. Reproducibility of retinal nerve fiber layer and macular thickness measurement with the RTVue-100 optical coherence tomograph. *Ophthalmology.* 2010;117:738–746.